Cancer Research

Global Downstream Pathway Analysis Reveals a Dependence of Oncogenic NF-E2–Related Factor 2 Mutation on the mTOR Growth Signaling Pathway

Tatsuhiro Shibata[1,2], Shigeru Saito[1,3], Akiko Kokubu[1], Takafumi Suzuki[4], Masayuki Yamamoto[4], and Setsuo Hirohashi[1,2]

Abstract

In multicellular organisms, adaptive responses to oxidative stress are regulated by NF-E2–related factor 2 (NRF2), a master transcription factor of antioxidant genes and phase II detoxifying enzymes. Aberrant activation of NRF2 by either loss-of-function mutations in the Keap1 gene or gain-of-function mutations in the Nrf2 gene occurs in a wide range of human cancers, but details of the biological consequences of NRF2 activation in the cancer cells remain unclear. Here, we report that mutant NRF2 induces epithelial cell proliferation, anchorage-independent growth, and tumorigenicity and metastasis *in vivo*. Genome-wide gene expression profiling revealed that mutant NRF2 affects diverse molecular pathways including the mammalian target of rapamycin (mTOR) pathway. Mutant NRF2 upregulates RagD, a small G-protein activator of the mTOR pathway, which was also overexpressed in primary lung cancer. Consistently, Nrf2-mutated lung cancer cells were sensitive to mTOR pathway inhibitors (rapamycin and NVP-BEZ235) in both *in vitro* and an *in vivo* xenograft model. The gene expression signature associated with mutant NRF2 was a marker of poor prognosis in patients with carcinoma of the head and neck region and lung. These results show that oncogenic Nrf2 mutation induces dependence on the mTOR pathway during carcinogenesis. Our findings offer a rationale to target NRF2 as an anticancer strategy, and they suggest NRF2 activation as a novel biomarker for personalized molecular therapies or prognostic assessment. *Cancer Res; 70(22); 9095–105. ©2010 AACR.*

Introduction

During the multistep carcinogenesis, cancer cells are exposed to multiple environmental stresses such as carcinogens, hypoxia, host inflammation, or anticancer drugs (1). They also have to deal with intrinsic stresses induced by genetic instability, oncogene-induced abnormal proliferation, or aberrant protein folding (1, 2). Therefore, acquisition of resistance to these stresses by some cancer cells would be beneficial for their survival, leading to malignant progression and lethal characteristics such as invasion, metastasis, and chemotherapy resistance (3). Oxidative stress in cancer is one of the important metabolic stresses caused by both extrinsic (reperfusion of a hypoxic microenvironment) and intrinsic (uncoupled mitochondrial activity) factors (4, 5). From the viewpoint of carcinogenesis, oxidative stress is a double-edged sword, because it promotes genetic alterations through DNA damage to drive malignant progression while also causing cell damage and inducing apoptosis (6, 7). Under physiologic conditions, cells possess molecular mechanisms that enable them to adapt to these stresses. In multicellular organisms, adaptive responses to oxidative stresses are regulated by NF-E2–related factor 2 (NRF2), a master transcription factor of many antioxidant genes and phase II detoxifying enzymes (8).

NRF2 belongs to the Cap'nCollar subfamily of basic leucine zipper (bZIP)–type transcriptional factors. It recognizes the specific antioxidant recognition element (ARE) sequence by forming a heterodimer with the bZIP family and promotes the expression of a wide range of cytoprotective genes (9). The activity of NRF2 is finely controlled by ubiquitin-mediated protein degradation. In unstressed cells, NRF2 is recognized by an E3 ubiquitin ligase, KEAP1, and rapidly degraded in the proteasome (10, 11). When cells are exposed to oxidative stress, the cysteine residues of KEAP1 are rapidly modified by electrophiles, resulting in structural change and loss of association with NRF2 (12). The free NRF2 released from KEAP1 then moves into the nucleus and induces its specific targets.

Previous studies have reported that NRF2 activation is beneficial for prevention of cancer, because *Nrf2*-deficient mice

Authors' Affiliations: [1]Cancer Genomics Project and [2]Pathology Division, National Cancer Center Research Institute; [3]Chem and Bio Informatics Department, Infocom Corporation, Tokyo, Japan and [4]Department of Medical Biochemistry, Tohoku University Graduate School of Medicine, Sendai, Japan

Corresponding Author: Tatsuhiro Shibata, Cancer Genomics Project, National Cancer Center Research Institute, 5-1-1, Tsukiji, Chuo-ku, Tokyo, 104-0045, Japan. Phone: 81-3-3547-5201 ext. 3123; Fax: 81-3-3248-2463; E-mail: tashibat@ncc.go.jp.

doi: 10.1158/0008-5472.CAN-10-0384

are susceptible to cancer development in chemical-induced carcinogenesis models and NRF2 promotes detoxification of carcinogen and decreases DNA damage by inducing phase II enzymes and reducing oxidative stressors such as reactive oxygen species (ROS), both mechanisms protecting normal cells from carcinogenesis (13, 14). However, recent studies have challenged this concept and shown that aberrant activation of NRF2 through either loss-of-function mutations in the *Keap1* gene or gain-of-function mutations in the *Nrf2* gene occurs in a wide range of human cancers such as lung (~40%), head and neck (~20%), gallbladder (~30%), liver, and breast cancers (15–20). Thus the KEAP1-NRF2 pathway seems to have a dual function in carcinogenesis, although the detailed biological consequences of NRF2 activation in cancer cells remain unknown.

Materials and Methods

Details of the experimental procedures are described in Supplementary Materials and Methods.

Cell biological analyses

Cell lines used in this study have been described previously (15, 16) and were validated by short tandem repeat genotyping. Rapamycin (Nakarai) and NVP-BEZ235 (LC Laboratories) were chemically synthesized and purchased. Mutant NRF2 cDNA and small interfering RNAs (siRNA; purchased from Thermo Fisher Scientific) were transfected into cells by using Lipofectamine and RNAiMAX (Invitrogen), and stable clones were isolated after G418 selection. Cell proliferation and drug sensitivity were measured by bromodeoxyuridine incorporation (cell proliferation ELIZA, Roche Diagnostic). All experiments were done in triplicate.

In vivo experiments

For *in vivo* assessment of mammalian target of rapamycin (mTOR) inhibitor, we transplanted 5×10^6 LK2 cells in the nude mice. NVP-BEZ235 (free base) was formulated in NMP/polyethylene glycol 300 (10:90, v/v). Solutions (5 mg/mL) were prepared fresh each day of dosing and were given daily (20 mg/kg) by oral gavage. The application volume was 10 mL/kg. Tumor volume was calculated by $(\text{tumor diameter})^2 \times (\text{tumor length}/2)$.

Molecular analyses

Total RNA was extracted from cell lines, primary squamous cell carcinoma (SCC) of the lung, and the corresponding normal lung tissues by RNAeasy (Qiagen). Quantitative reverse transcription-PCR (RT-PCR) was performed in triplicate and evaluated using universal probes for each amplicon and the Light-Cycler system (Roche Diagnostic). Protein extraction and immunoblotting were performed as described previously (15). Antibodies and siRNA used in this study were listed in Supplementary Table S1.

Microarray analysis of global gene expression

Ten micrograms of total RNA were reverse-transcribed by Moloney murine leukemia virus reverse transcriptase, and a Cy3-labeled cRNA probe was synthesized using T7 RNA polymerase in accordance with the manufacturer's protocol. Probes were hybridized with a microarray containing 41,000 oligonucleotides covering the whole human genome (Whole Human Genome Oligo Microarray, G4112F, Agilent Technologies). All analyzed microarray data are in accordance with the MIAME guidelines.

Statistical analysis

Among the total of 41,000 probes, 12,091 stable probes corresponding to the MAQC common genes were used for statistical analysis. To characterize the molecular backgrounds of the gene list, enrichment analysis for Gene Ontology (GO) was performed using the GO Term Finder (http://go.princeton.edu/cgi-bin/GOTermFinder). Preranked gene set enrichment analysis was applied for the gene list with C2 pathway gene sets and 2,000 permutations (http://www.broadinstitute.org/gsea/index.jsp). Two independent sets of gene expression data from head and neck cancer and squamous lung cancer were classified into two groups based on the signatures of the gene list using *K*-means clustering (R cluster package). Then, stable clusters were obtained in 1,000 random trials to avoid artifacts of classification due to dependency of initial random seeds. Survival analysis was performed using the Kaplan-Meier method, and log-rank test was used to evaluate disease-free survival.

Results

Oncogenic phenotypes of HEK293 cells expressing mutant NRF2

We established stable HEK293 (an immortalized human epithelial cell line) clones expressing two mutant NRF2 cDNAs (T80R and L30F mutants), both of which were detected in human cancer and behave as gain-of-function mutants (15). Clones expressing mutant and wild-type NRF2 cDNA showed accumulation of NRF2 in the nuclear fraction of these clones (Fig. 1A, top). The degree of nuclear NRF2 accumulation in these clones (samples 3 and 4) was less than the endogenous NRF2 accumulation in *Nrf2*- (sample 6) or *Keap1*- (sample 5) mutated cancer cell lines (refs. 15, 16; Fig. 1A, bottom).

We then tested the cell proliferation activity and found that clones expressing mutant NRF2 grew more rapidly than the mock or wild-type NRF2-transfected clones (especially T80R mutants; Fig. 1B). Downregulation of NRF2 by siRNA inhibited the proliferation of clones stably expressing the mutant and wild-type NRF2 gene, whereas growth of the mock control was little affected (Supplementary Fig. S1A and B). We also tested the anchorage-independent cell growth of these clones. As shown in Fig. 1C, both mutant NRF2-expressing clones produced colonies in soft agar, whereas the control clone formed no colonies. In addition, NRF2 mutant clones showed an increase of cell migration activity *in vitro* (Fig. 1D). We had previously reported two lung cancer cell lines (EBC1 and LK2) that harbored the *Nrf2* mutation (EBC1 cell has the D77V mutation, and LK2 cell has the E79K mutation; ref. 15). Downregulation

of NRF2 also reduced the proliferation of *Nrf2* mutant cancer cells but exerted no effect on SQ5 cells that contain low wild-type NRF2 protein (Fig. 1A; Supplementary Fig. S1C and D), supporting the contention that *Nrf2*-mutated cancer cells depend on the Nrf2 activity for their proliferation as previously reported in *Keap1*-mutated cancer cells (17).

We further examined the *in vivo* tumorigenic activity of mutant NRF2-expressing cells by s.c. transplantation in immunodeficient mice. Both clones expressing mutant NRF2 produced tumors at markedly high frequency, whereas control clones did not form tumors (TR-1: 8/8, TR-2: 8/8, LF1: 5/8, LF2: 7/8, control: 0/10; Fig. 2A; Supplementary Table S2). Tumors expressing mutant NRF2 exhibited poorly differentiated carcinoma with increased mitotic activity (>70% cells being immunopositive for Ki67; Fig. 2B and C), accompanied in most cases by highly aggressive characteristics, such as invasion into the surrounding adipose and muscle tissues (Fig. 2D). Moreover, there was occasional metastasis to the liver, suggesting that mutant NRF2 confers invasive and metastatic activity (Fig. 2E and F), consistent with the increased cell migration activity observed *in vitro* (Fig. 1D). We also noted that these tumors contained many microvessels (as revealed by CD34 staining; Fig. 2B and G). As observed under *in vitro* culture conditions, the tumor cells overexpressed a NRF2 target, NQO1 *in vivo* (Fig. 2H).

Gene expression profiling of HEK293 cells expressing mutant NRF2

Because NRF2 encodes a sequence-specific transcriptional factor, direct or indirect downstream targets of NRF2 should contribute to at least a proportion of the phenotypes described above. We attempted to overview the genome-wide changes in gene expression induced by mutant NRF2 and conducted a microarray analysis (Fig. 3A). Among individual

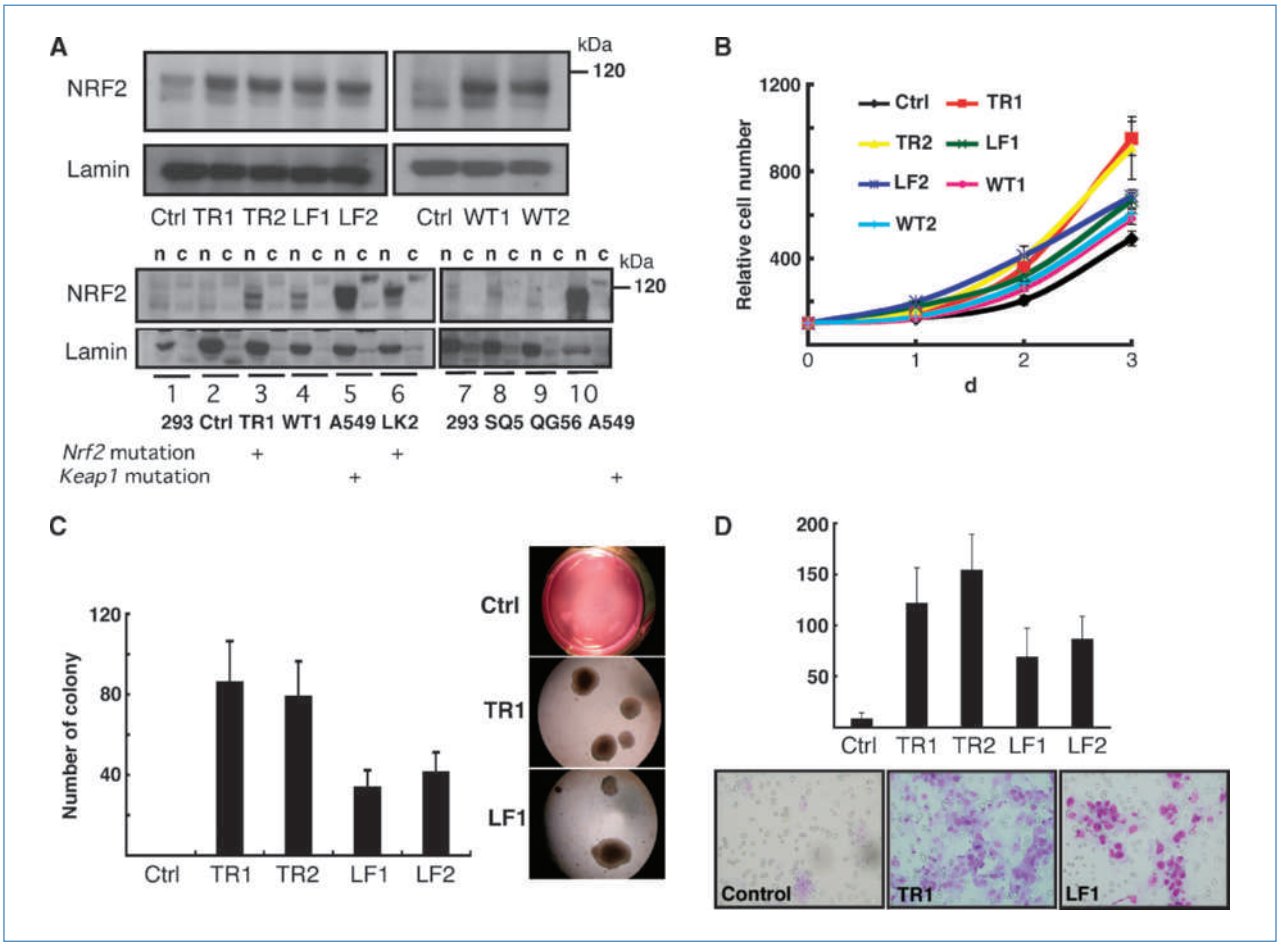

Figure 1. Mutant NRF2 confers oncogenic phenotypes *in vitro*. A, top, accumulation of nuclear NRF2 in clones expressing mutant (left) and wild (right) NRF2. The nuclear extract of each clone was blotted with anti-NRF2 antibody. Bottom, NRF2 protein expression in established clones was compared with endogenous NRF2 accumulation in *Nrf2*-mutated (LK2), *Keap1*-mutated (A549), and both wild (SQ5 and QG56) cancer cell lines. Nuclear (n) and cytplasmic (c) fractions were separately examined. Lamin B1 was used as a loading control. Molecular marker is indicated on the right (kDa). B, increased proliferation of mutant and wild-type NRF2-expressing clones compared with the mock control. Relative number of the cells in each clone was measured and plotted (n = 3). C, clones expressing mutant NRF2 showed anchorage independence growth in the soft agar assay (n = 4 in each clone). Representative pictures of agar wells are shown (left). D, clones expressing mutant NRF2 exhibited elevated migratory activity. The average number of migrated cells (n = 6 in each clone). Representative micrographs of transwells are shown at the bottom. Data represent the mean ± SD.

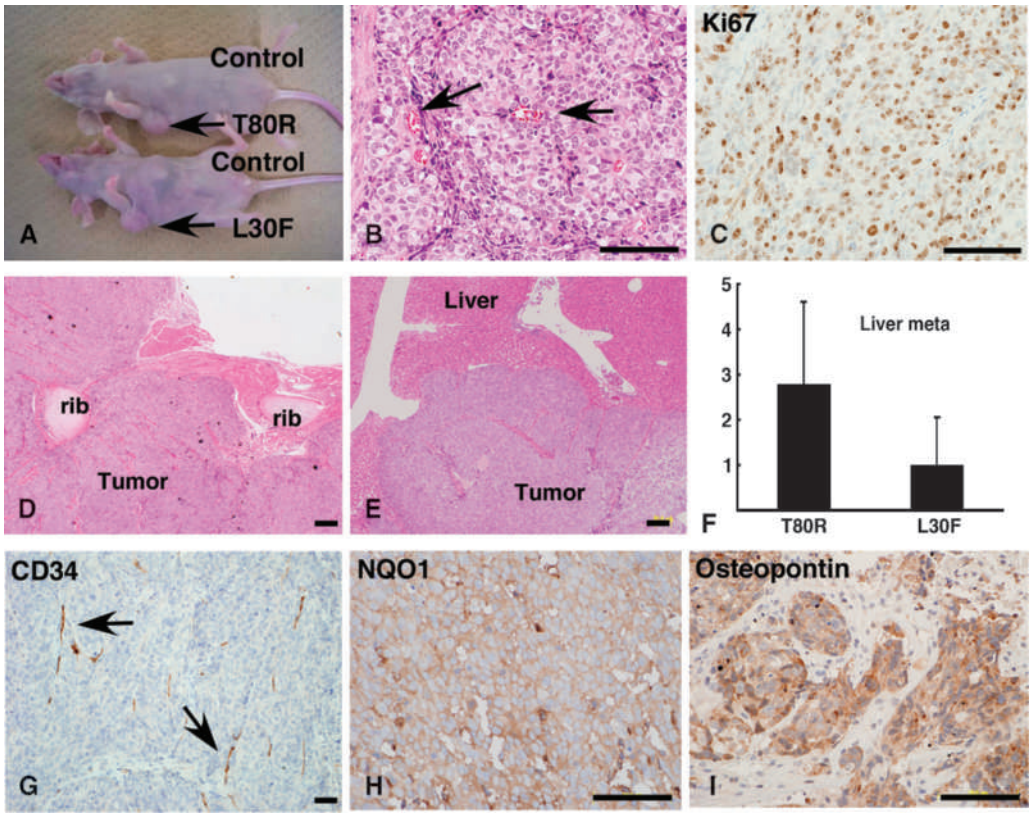

Figure 2. Mutant NRF2 confers oncogenic phenotypes *in vivo*. A, representative view of mice bearing transplants (top, TR1 and mock; bottom, LF1 and mock). B-D, histologic appearance (H&E staining) of tumors formed by clones expressing mutant NRF2. B, the tumors showed solid growth with induction of small vessels (arrows). C, high mitotic activity of tumor cells detected by Ki67 staining. D, local invasion of tumors. Tumor cells directly invaded to the muscle tissues around the rib. E, liver metastasis of tumors. F, the number of metastatic nodules in the liver of mice harboring tumors (mean ± SD, n = 16 in TR clones and n = 12 in LF clones). G, detection of tumor-associated small vessels by CD34 staining. H, prominent cytoplasmic expression of NQO1, a NRF2 target, in tumors. I, detection of osteopontin expression in tumor cells. Bar, 100 μm.

downstream genes, we observed upregulation of several antioxidant genes (Nqo1, Hmox1, Abcc2, and enzymes relating to glutathione synthesis) that have been previously reported to be NRF2 target genes, and we validated the increased expression of these authentic targets by quantitative RT-PCR (Supplementary Fig. S2A and B). Among the other downstream targets, we also observed increased expression of osteopontin, which has been reported to be associated with metastatic activity and angiogenesis in cancer (21, 22), both *in vitro* and *in vivo* (Supplementary Fig. S1C; Fig. 2I). We also detected direct NRF2 binding in the promoter of the onsteopotin gene by chromatin immunoprecipitation (ChIP) sequencing.[5]

GO analyses of control and mutant NRF2-expressing clones revealed that persistent expression of mutant NRF2 affected multiple signal pathways (Supplementary Table S3). Consistent with its previously known roles in the adaptative response to oxidative stress, mutant NRF2 significantly induced genes belonging to categories such as "response to stress" and "response to chemical stimuli." In addition, expression of genes related to inflammatory processes ("response to wounding," "defense response," "inflammatory response," and "cytokine production") and cell motility ("locomotor behavior" and "chemotaxis") was also altered in NRF2 mutant clones.

Prognostic significance of the mutant NRF2 signature in human cancer

Because mutant NRF2 promoted cell proliferation and anchorage-independent growth *in vitro* and metastasis activity and increased angiogenesis *in vivo*, which are all hallmarks of cancer malignancy, the molecular signature induced by mutant NRF2 may be associated with poor clinical outcome. To test this hypothesis, we extracted the mutant NRF2 signature (complete gene list is shown in Supplementary Table S4) and examined its association with clinical data using archives of previous microarray data. We first analyzed a large cohort (n = 60) of head and neck cancer samples (23) because NRF2 is frequently mutated in this type of cancer, and thus far little information has been

[5] M.Y. and Yoichiro Mitsuishi, unpublished observation.

available about its prognostic molecular signature. On the basis of the mutant NRF2 signature, we classified the samples into two clusters (Cluster1, n = 45; Cluster 2, n = 15; Fig. 3B) and compared the prognosis between them. As shown in Fig. 4B, cases containing the mutant NRF2 signature showed significantly poorer prognosis (P = 0.000118), supporting the contention that the gene profile extracted from HEK293 cells is comparable with the malignant signature of clinical SCC samples. To validate this result, we then analyzed another cohort of lung SCC cases (24). Although the difference did not reach statistical significance (P = 0.0803), probably because of the small size of the cohort (n = 16), we observed a trend for tumors harboring the mutant NRF2 signature to have a poorer prognosis than those without the signature (Supplementary Fig. S3).

Identification of molecular pathways regulated by mutant NRF2

To further elucidate the molecular pathways affected by mutant NRF2, we then conducted gene set enrichment analysis (GSEA). This revealed significant enrichment of several pathways in clones expressing mutant NRF2 (Table 1; all significant pathways are listed in Supplementary Table S5). Consistent with the above GO analysis, we detected significant enrichment of pathways associated with genes induced by oxidative stresses such as ROS (Houstis_ROS) or UV treatment (UVB_SCC_UP, UVB_NHEK3_C0, UVB_NHEK3_C3, and UVB_NHEK3_ALL). Another noteworthy finding was that the molecular signature induced by mutant NRF2 included pathways associated with mTOR signaling (Peng_Rapamycin_DN, Peng_Leucine_DN, Peng_Glutamine_DN; ref. 25; Fig. 3C). We also observed other molecular pathways associated with other stresses (hypoxia or viral infection), the progenitor cell signature, and lipid metabolism (Supplementary Fig. S4). Thus, it was revealed that mutant NRF2 induced a set of genes more diverse than had previously been thought. In particular, the mTOR pathway emerged as a new target of NRF2, in addition to various stress-regulated genes.

Activation of the mTOR pathway by mutant NRF2

Because the mTOR pathway has been reported to be an attractive therapeutic target in many solid tumors, we then focused on the relationship between the NRF2 and mTOR pathways. We first examined activation of the mTOR pathway in HEK293 clones expressing mutant NRF2. Immunoblot analysis revealed increased phosphorylation of ribosomal S6

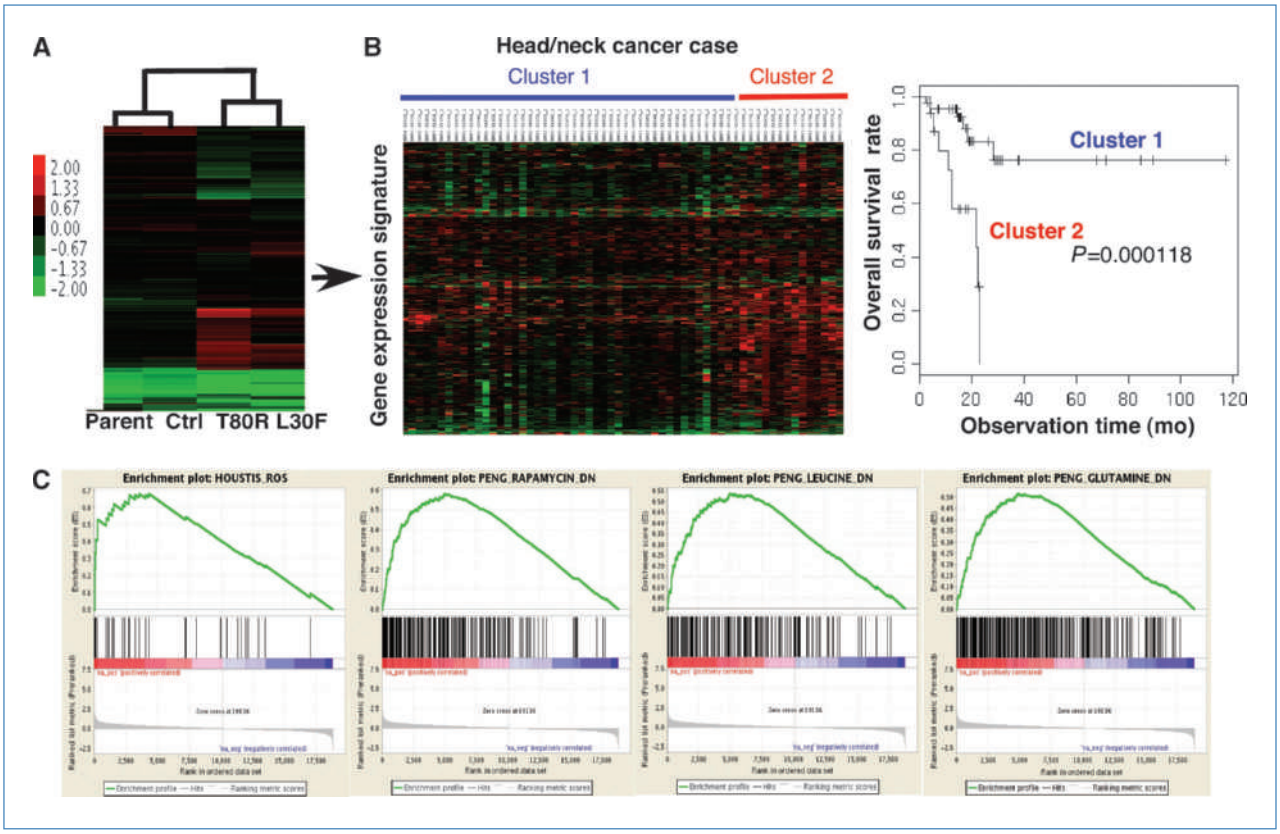

Figure 3. Gene expression profiling of cells expressing mutant NRF2. A, two-dimensional hierarchal clustering of parent, mock, and clones expressing mutant NRF2 by genome-wide gene expression. B, heat map of primary head and neck cancers based on *K*-means clustering using the mutant NRF2 gene expression signature (left). Kaplan-Meier analysis of a head and neck cancer cohort segregated by the mutant NRF2 gene expression signature (right). Cases expressing that signature showed significantly worse prognosis. C, representative panels showing results of gene set enrichment analysis of genes regulated by mutant NRF2.

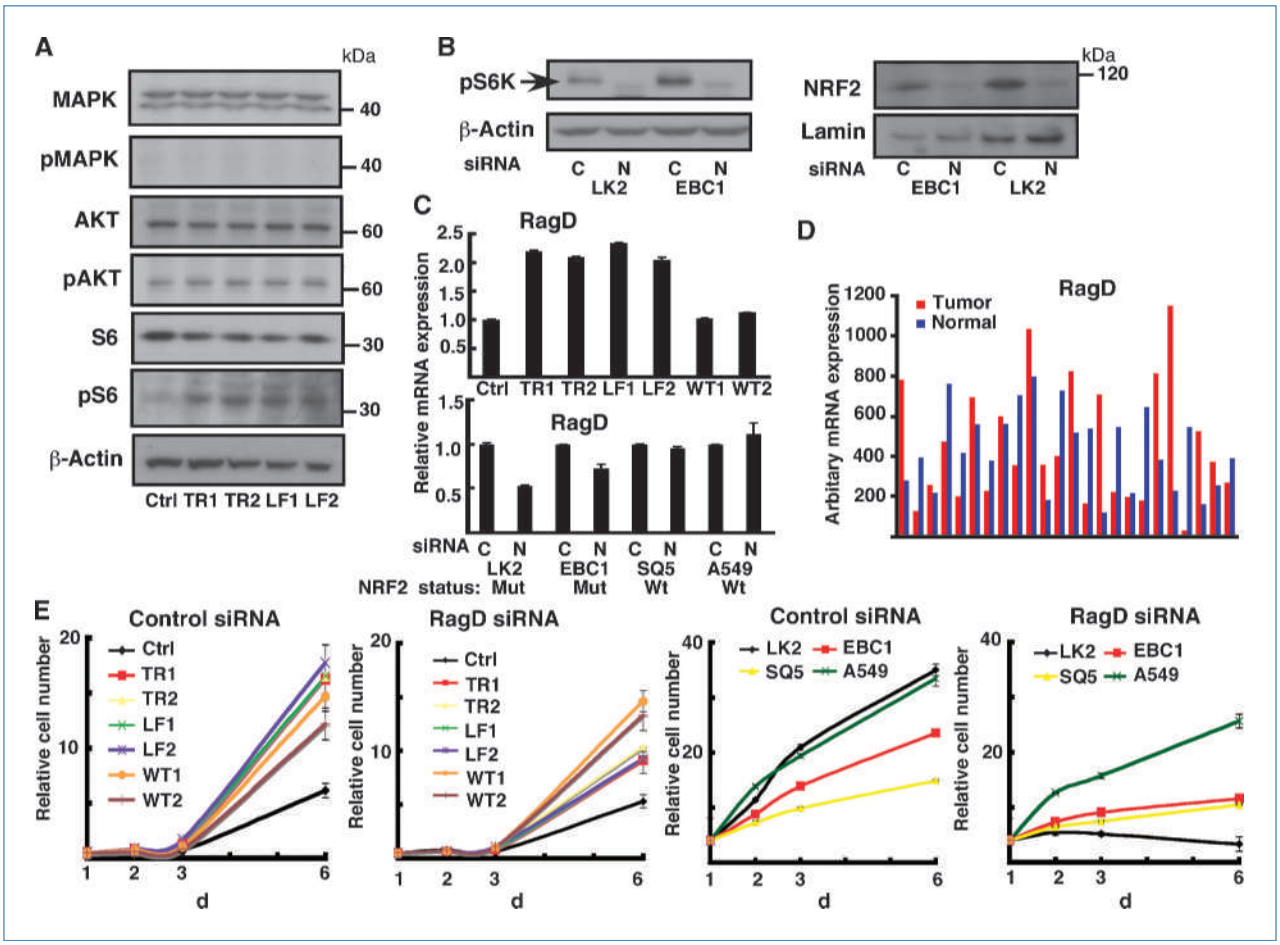

Figure 4. Activation of the mTOR pathway and increase of RagD expression by mutant NRF2. A, immunoblot analysis revealed increased phosphorylation of S6 in mutant NRF2-expressing clones compared with the mock control. B, *Nrf2*-mutated cancer cell lines were treated with control siRNA (C) and NRF2 siRNA (N), and S6 kinase phosphorylation (left) and NRF2 expression (right) were examined. C, left, upregulation of RagD expression in mutant NRF2-expressing clones (top). Reduced expression of RagD in NRF2-downregulated cancer cells compared with the control siRNA treatment (bottom). Right, quantitative measurement of RagD mRNA expression in primary lung SCC and corresponding normal lung tissue. D, proliferation of mutant NRF2-expressing clones and *Nrf2*-mutated cancer cells treated with control and RagD siRNAs. Data represent the mean ± SD ($n = 3$). β-Actin and lamin B1 were used as loading controls. Molecular marker is indicated on the right (kDa).

protein, which encodes one of the major downstream substrates of the mTOR pathway, and a mild increase of AKT phosphorylation in mutant NRF2-expressing cells relative to the control, whereas no strong activation of mitogen-activated protein kinase was observed in any of the clones (Fig. 4A). Downregulation of NRF2 expression in *Nrf2*-mutated cancer cells was associated with reduced S6 kinase activation (Fig. 4B).

To understand the molecular link between the two pathways, we returned to the gene expression profiling because NRF2 is a transcriptional factor and does not seem to interact directly with mTOR signaling. We searched for the downstream targets of mutant NRF2, which are responsible for modulating the mTOR pathway. Among the genes whose expression was found to be significantly altered in the microarray analysis, we found that a member of the small G protein family, RagD, which encodes a recently discovered activator of the mTOR pathway (26), was significantly upregulated in the HEK293 cells expressing mutant NRF2 (Fig. 4C). RagD knockdown reduced the activation of mTOR signaling (Supplementary Fig. S5) and NRF2 downregulation reduced RagD expression in *Nrf2*-mutated cancer cells (Fig. 4C). The expression of RagD was also quantified in the clinical samples of primary lung SCC and increased in >40% (10 of 24, 41.7%) of tumors relative to corresponding normal lung tissue (Fig. 4C). We found that cell proliferation of both mutant NRF2 expression HEK293 clones and *Nrf2*-mutated cancer cells was reduced by downregulation of RagD expression (Fig. 4D; Supplementary Fig. S6). Collectively, therefore, mutant NRF2 upregulates RagD expression and RagD plays an important role in the proliferation of *Nrf2*-mutated cancer cells.

mTOR pathway dependence of cell survival in NRF2 mutant cancer

These results prompted us to examine whether inhibition of the mTOR pathway has any effect on *Nrf2* mutant cancer.

We first examined whether the proliferation of clones expressing mutant NRF2 was sensitive to inhibition of the mTOR pathway. We treated mutant NRF2-expressing HEK293 clones with rapamycin, a small-molecule inhibitor of mTOR, and measured the resulting cell proliferation. As shown in Fig. 5A, rapamycin treatment more effectively reduced cell proliferation in *Nrf2* mutant clones than in the mock and wild-type NRF2-expressing ones (IC_{50} values: control >10 nmol/L, TR1 0.29 nmol/L, TR2 0.3 nmol/L, LF1 0.34 nmol/L, LF2 0.53 nmol/L, WT1 9.94 nmol/L, WT2 >10 nmol/L). We then tested low wild-type NRF2 expressing (SQ5 and QG56), high wild-type NRF2-expressing (A549), and high mutant NRF2-expressing (LK2 and EBC1) cancer cell lines (Fig. 1A). *Nrf2* mutated cancer cell lines exhibited more sensitivity to rapamycin than did *Nrf2* wild-type cancer cell lines (Fig. 5A). However, *Nrf2* mutant cells showed resistance to rapamycin at a higher dose, probably because of the more transformed phenotypes such as feedback system involving phosphoinositide 3-kinase (PI3K) reported previously in other cancer cells (27, 28). Consistently high-dose (1 nmol/L) rapamycin treatment did not robustly reduce the phosphorylation of mTOR pathway targets in LK2 and EBC1 cells (Fig. 5B). To overcome this resistance in cancer cells, we then tested a dual kinase inhibitor (NVP-BEZ235), which targets both mTOR and PI3K and is currently being evaluated in clinical trials. NVP-BEZ235 robustly inhibited mTOR pathway activation and significantly reduced the cell proliferation of *Nrf2*-mutated lung cancer cells (Fig. 5A and B; IC_{50} values: LK2 0.042 μmol/L, EBC1 0.099 μmol/L, SQ5 >5 μmol/L, QG56 >5 μmol/L, A549 >5 μmol/L). Similar drug sensitivity was also observed in an *Nrf2*-mutated head and neck cancer cell line (HO-1-U1; data not shown). NVP-BEZ235 also induced apoptosis in *Nrf2*-mutated cancer cells as revealed by an increase in the expression of cleaved poly(ADP-ribose) polymerase (PARP; Fig. 5B). Finally, we challenged an *in vivo* treatment model with NVP-BEZ235. NVP-BEZ235 was administered p.o. to mice bearing s.c. xenografts of LK2 or SQ5 cells, and we

Table 1. Gene signatures associated with mutant NRF2 expression

Gene signature	Corrected *P*	FDR (%)	Associated pathway
Peng_Rapamycin_DN	0	0	mTOR pathway
Houstis_ROS	0	0	Oxidative stress
Park_RARALPHA_MOD	0	0.002	
PGC	0	0.012	Lipid metabolism
UVB_SCC_UP	0	0.011	Oxidative stress
KREBS_TCA_CYCLE	0	0.013	Metabolic signal
Halmos_CEBP_UP	0	0.016	Lipid metabolism
UVB_NHEK3_C0	0	0.016	Oxidative stress
Zucchi_Epithelial_UP	0.001	0.018	Cancer
Peng_Leucine_DN	0	0.016	mTOR pathway
Addya_K562_HEMIN_Treatment	0	0.016	
Peng_Glutamine_DN	0	0.016	mTOR pathway
HSA00100_Biosynthesis_OF_Steroids	0	0.02	Lipid metabolism
TCA	0.001	0.02	Metabolic signal
Cholesterol_Biosynthesis	0	0.022	Lipid metabolism
IDX_TSA_UP_Cluster5	0	0.022	Lipid metabolism
Rutella_HEPATGFSNDCS_UP	0	0.021	
Hypoxia_RCC_NOVHL_UP	0	0.029	Hypoxia
Flechner_Kidney_Transplant_Well_PBL_UP	0	0.036	
SIG_CD40PathwayMap	0	0.036	TNF/NF-κB/virus
UVB_NHEK3_C3	0	0.034	Oxidative stress
P53Hypoxiapathway	0.002	0.037	Hypoxia
Tarte_Plasma_Blastic	0	0.039	Progenitor cell
UVB_NHEK2_DN	0	0.038	Oxidative stress
TSA_Hepatoma_Cancer_DN	0.004	0.037	Cancer
Ubiquitin_Mediated_Proteolysis	0	0.037	Metabolic signal
Wieland_Hepatitis_B_Induced	0	0.037	TNF/NF-κB/virus
HSC_LaterProgenitors_Adult	0	0.036	Progenitor cell
CMV_HCMV_Time Course_24HRS_DN	0.002	0.038	TNF/NF-κB/virus
UVB_NHEK3_ALL	0	0.041	Oxidative stress

Abbreviation: FDR, false discovery rate.

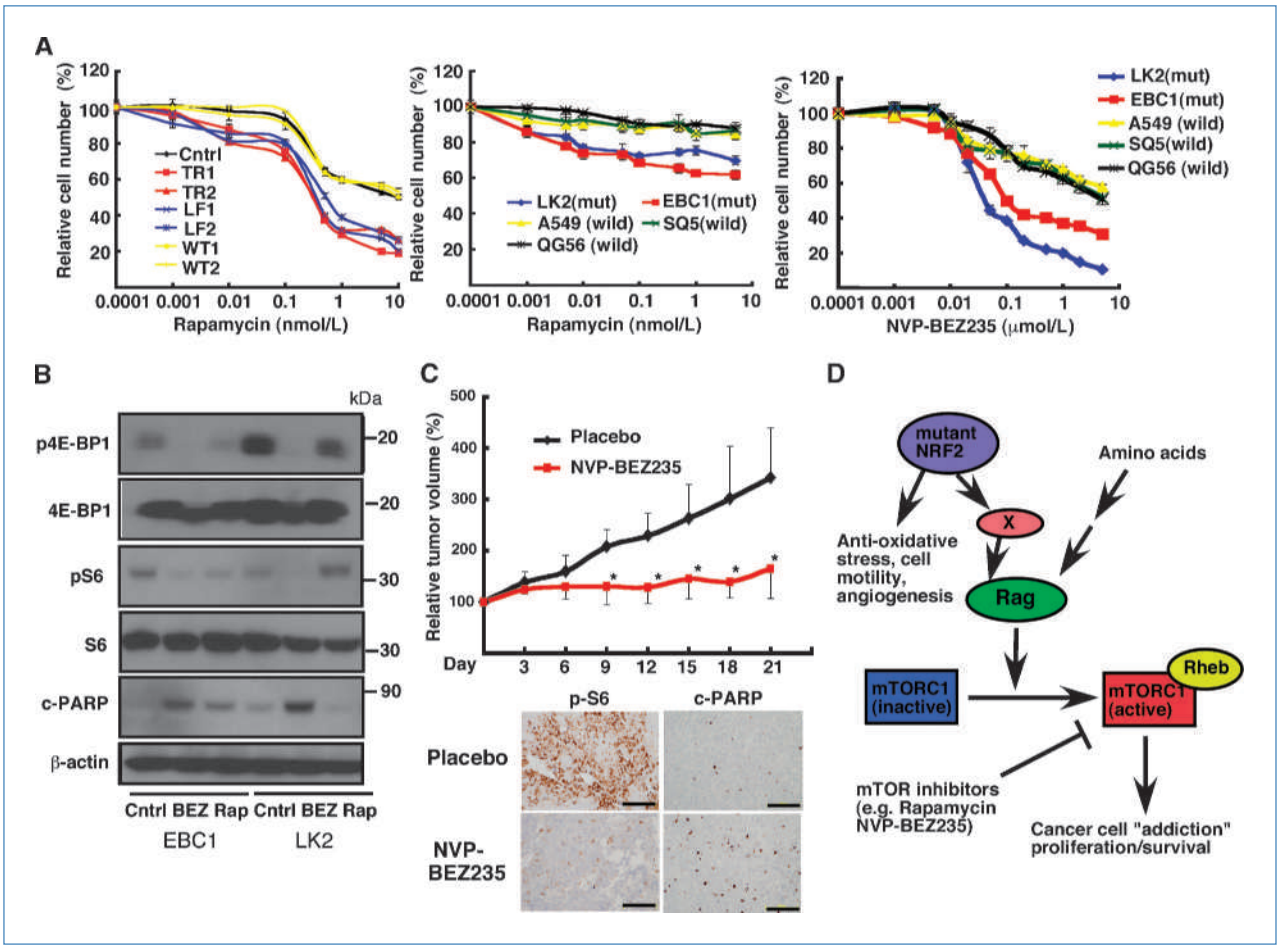

Figure 5. mTOR pathway dependence of cell survival in NRF2 mutant cancer. A, left, clones expressing mutant (TR and LF) and wild-type (WT) NRF2 or mock were treated with different concentrations of rapamycin, and the number of viable cells was measured after 3 d and plotted. Middle, *Nrf2*-mutated cancer cells (LK2 and EBC1) and *Nrf2* wild-type cancer cells (A549, SQ5, and QG56) were treated with rapamycin in a similar way, and the number of viable cells was plotted. Right, *Nrf2*-mutated and *Nrf2* wild-type cancer cells were treated with different concentration of NVP-BEZ235, a dual inhibitor of mTOR and PI3K, and viable cell number was measured and plotted. B, cancer cells were treated with DMSO (Ctrl), 0.5 μmol/L NVP-BEZ235 (BEZ), and 1 nmol/L rapamycin (Rap) for 48 h, and phosphorylation of S6 and 4E-BP1 was examined. Cleaved PARP (C-PARP) was examined as an indicator of apoptosis. Total 4E-BP1, S6, and β-actin were used as loading controls. Molecular marker is indicated on the right (kDa). C, top, immunodeficient mice, which contained s.c. LK2 tumors, were randomly segregated into two groups. NVP-BEZ235 was daily given to mice in the treated group (n = 8), whereas placebo was given to the control group (n = 8) for 3 wk. The relative tumor size in each group was plotted. *, $P < 0.001$. Bottom, decrease in phospho-S6 protein and increase in cleaved PARP in NVP-BEZ235 treated tumor (right) compared with the control (left). Bar, 100 μm. D, schematic representation of mTOR pathway dependence in *Nrf2*-mutated cancer. Data represent the mean ± SD (n = 3, except in D).

found that this drug significantly inhibited the growth of LK2 cells in comparison with placebo treatment (Fig. 5C). Immunohistologic analysis confirmed significant inhibition of mTOR activation (indicated by decreased phospho-S6) and induction of apoptosis (increase of cleaved PARP and caspase-3 activation) in NVP-BEZ235–treated LK2 tumors relative to the placebo-treated ones (Fig. 5C; Supplementary Fig. S7).

Discussion

In this study, we found that mutant NRF2 confers improved cell proliferation, anchorage-independent growth, and *in vivo* tumorigenicity, which are the fundamental hallmarks of an oncogene, in an immortalized human epithelial cell line. Moreover, cells expressing mutant NRF2 showed malignant phenotypes such as enhanced local invasion and metastasis to distant organ. These phenotypes could be explained by acquisition of resistance to or reduction of the oxidative stress induced by the intrinsic cellular immortalization process and extrinsic environmental factors *in vivo,* but our gene expression analysis revealed that mutant NRF2 affects a broader range of biological processes in addition to the antioxidant pathway.

The aforementioned results imply that mutant NRF2 directly or indirectly regulates a set of genes related to the carcinogenesis process. To clarify this transcriptional network and identify therapeutic targets in *Nrf2*-mutated cancer, we

performed gene expression profiling and conducted "pathway analysis" to connect the expression patterns of gene groups with specific phenotypes. This analysis revealed that, in addition to the previously known NRF2 targets, mutant NRF2 altered the expression of a battery of genes, many of which had not been previously assigned to the oxidative stress pathway, in human epithelial cells. This result partly overlaps (e.g., genes related to lipid metabolism) with the previous gene expression analyses of *Keap1*-deleted mouse hepatocytes (29, 30) and our findings of a genome-wide study to clarify the *in vivo* sites of NRF2 binding to chromatin in *Keap1* mutated cancer cells.[6] To delineate the molecular pathways affected by mutant NRF2, we performed GSEA (31) and discovered significant enrichment of genes associated with the mTOR pathway, lipid metabolism, and other cellular stresses such as hypoxia and viral infection.

The finding that mutant NRF2 is implicated in the mTOR pathway had not been anticipated. This relationship is also strengthened by the fact that NRF2 mutant–expressing clones and cancer cells are sensitive to mTOR pathway inhibitors (rapamycin and NVP-BEZ235). The mTOR pathway sensitizes cells to changes in multiple extracellular signals/environments (depletion of growth factors and nutrients or cellular stresses such as hypoxia and DNA damage) and dynamically regulates translation, ribosome biogenesis, macroautophagy, and other processes (32, 33); thus, it would be possible that NRF2-mediated stress adaptation may converge with this environmental sensing system. To determine how NRF2 modulates the mTOR pathway, we focused on the gene expression data and have revealed one candidate, RagD, which is a positive regulator of the mTOR pathway (33, 34) and was induced by mutant NRF2. RagD is a member of the small G-protein family and enhances mTOR activity through direct binding and by recruiting the mTOR complex to the endosomal fraction (26), where mTOR is activated by Rheb, another small G protein, which has been shown to be an oncogene in a mouse model as well as in chick fibroblasts (35, 36). Although the expression of RagD was increased in primary lung cancers, the transcriptional regulation of the Rag gene family has been largely unexplored; it has only been reported that amino acid addition triggers its activation (26). RagD expression in cancer samples was significantly associated with Hmox1, another Nrf2 target gene ($P = 0.025$; Supplementary Fig. S8). However, the putative promoter region of the RagD gene contains no ARE sequence and our chromatin immunoprecipitates sequence (ChIP-seq) analysis has revealed that RagD is not a direct target of NRF2 (data not shown). These findings suggest that an additional regulatory mediator links the two molecules (Fig. 5D).

Continuous NRF2 activation probably stimulates the mTOR pathway on which cancer cells have become dependent, making it a potential therapeutic target. Identification of such indirect molecular addiction has been recently reported as NF-κB activation in *Kras/Tp53* mutated cancer cells (37) and could expand a window of anticancer therapeutic strategy especially when targeting oncoproteins encoding transcriptional factors. Recently, mTOR inhibitors have caught much attention as promising anticancer drugs (38, 39). Previous studies elucidated the existence of feedback mechanism against mTOR inhibitors in cancer (27, 28) and a dual kinase inhibitor (NVP-BEZ235), which targets both the mTOR and PI3Ks, has been recently shown to be more effective in many solid tumors, including *Kras* mutated lung cancer or *Pik3ca* mutated cancers (40–42). The present study also supports that the dual kinase inhibition would be beneficial in treating *Nrf2* mutated cancer. However, it remains unclear how mutant NRF2 activates AKT in the presence of the negative feedback and further studies to uncover the molecular interaction of NRF2 and PI3K/AKT/mTOR signaling would be required. Notably, we reported that *Nrf2* mutation occurs more frequently in lung cancers without *Egfr* and *Kras* mutations (15). Therefore, the mTOR pathway may also be a promising therapeutic target in the *Nrf2*-mutated subtype of lung cancer.

Mutant NRF2 promoted cell motility, local invasion, angiogenesis, and liver metastasis. GO profiling also revealed significant enrichment of genes related to cell motility. Previous studies have shown that upregulation of osteopontin, an extracellular matrix-associated protein with multiple functional domains, is associated with metastatic activity of a range of cancers including head and neck and lung cancers (21, 43) and enhancement of angiogenesis (22). We found that osteopontin was highly expressed in cells expressing mutant NRF2 and that NRF2 seems to directly activate the osteopontin gene. In addition to osteopontin, mutant NRF2 induced a battery of genes such as matrix metalloproteinase 12 and heparin-binding epidermal growth factor-like growth factor, which are associated with tumor metastasis (44, 45). Thus NRF2-mediated adaptation to environmental stress seems to be tightly associated with tumor metastasis and progression. Because our experimental model showed that the presence of mutant NRF2 confers metastatic potential, the molecular signature resulting from NRF2 activation may be associated with poor outcome in clinical cases. We tested this hypothesis and confirmed that the mutant NRF2 signature is indeed a prognostic factor in SCC of the head and neck region and probably that of the lung. Interestingly, an independent study focusing on the prognostic molecular pathway in lung adenocarcinoma has identified the Peng_Rap_DN pathway, a top-ranking gene set enriched in mutant NRF2 clones, as a signature that is significantly associated with poor prognosis (46). This also supports our contention that the mutant NRF2 signature is a marker of poor prognosis.

In conclusion, our results show the existence of an intimate association between oxidative stress and the mTOR pathway in cancer and further highlight the potential of NRF2 activation as a novel biomarker for personalized molecular therapies or prognostic assessment. From a clinical viewpoint, it is important to note that NRF2 activation in cancer is significantly associated with response to anti-mTOR pathway treatments, which are being widely investigated in clinical trials for many cancers.

[6] M.Y. and colleagues in preparation.

Disclosure of Potential Conflicts of Interest

No potential conflicts of interest were disclosed.

Grant Support

A grant-in-aid for the Comprehensive 10-Year Strategy for Cancer Control, Ministry of Health, Labor and Welfare, Japan grant-in-aid for cancer research 19-1, Princess Takamatsu Cancer Research Fund research grant 08-24007, and Program for Promotion of Fundamental Studies in Health Sciences of the National Institute of Biomedical Innovation, Japan.

The costs of publication of this article were defrayed in part by the payment of page charges. This article must therefore be hereby marked *advertisement* in accordance with 18 U.S.C. Section 1734 solely to indicate this fact.

Received 01/30/2010; revised 09/15/2010; accepted 09/21/2010; published OnlineFirst 11/09/2010.

References

1. Bartkova J, Rezaei N, Liontos M, et al. Oncogene-induced senescence is part of the tumorigenesis barrier imposed by DNA damage checkpoints. Nature 2006;444:633–7.
2. Whitesell L, Lindquist SL. HSP90 and the chaperoning of cancer. Nat Rev Cancer 2005;5:761–72.
3. Luo J, Solimini NL, Elledge SJ. Principles of cancer therapy: oncogene and non-oncogene addiction. Cell 2009;136:823–37.
4. Jolly C, Morimoto RI. Role of the heat shock response and molecular chaperones in oncogenesis and cell death. J Natl Cancer Inst 2000; 92:1564–72.
5. Singh KK. Mitochondrial dysfunction is a common phenotype in aging and cancer. Ann N Y Acad Sci 2004;1019:260–4.
6. Mena S, Ortega A, Estrela JM. Oxidative stress in environmental-induced carcinogenesis. Mutat Res 2009;674:36–44.
7. Gottlieb E, Tomlinson PM. Mitochondrial tumour suppressors: a genetic and biochemical update. Nat Rev Cancer 2005;5:857–66.
8. Motohashi H, Yamamoto M. Nrf2-1 defines a physiologically important stress response mechanism. Trends Mol Med 2004;10: 549–57.
9. Itoh K, Chiba T, Takahashi S, Ishii T, et al. An Nrf2/small Maf heterodimer mediates the induction of phase II detoxifying enzyme genes through antioxidant response elements. Biochem Biophys Res Commun 1997;236:313–22.
10. Itoh K, Wakabayashi N, Katoh Y, et al. Keap1 represses nuclear activation of antioxidant responsive elements by Nrf2 through binding to the amino-terminal Neh2 domain. Genes Dev 1999;13:76–86.
11. McMahon M, Itoh K, Yamamoto M, et al. Keap1-dependent proteasomal degradation of transcription factor Nrf2 contributes to the negative regulation of antioxidant response element-driven gene expression. J Biol Chem 2003;278:21592–600.
12. Yamamoto T, Suzuki T, Kobayashi A, et al. Physiological significance of reactive cysteine residues of Keap1 in determining Nrf2 activity. Mol Cell Biol 2008;28:2758–70.
13. Ramos-Gomez M, Kwak MK, Dolan PM, et al. Sensitivity to carcinogenesis is increased and chemoprotective efficacy of enzyme inducers is lost in nrf2 transcription factor-deficient mice. Proc Natl Acad Sci U S A 2001;98:3410–5.
14. Aoki Y, Hashimoto AH, Amanuma K, et al. Enhanced spontaneous and benzo(a)pyrene-induced mutations in the lung of Nrf2-deficient gpt δ mice. Cancer Res 2007;67:5643–8.
15. Shibata T, Ohta T, Tong KI, et al. Cancer related mutations in NRF2 impair its recognition by Keap1-3 E3 ligase and promote malignancy. Proc Natl Acad Sci U S A 2008;105:13568–73.
16. Shibata T, Kokubu A, Gotoh M, et al. Genetic alteration of Keap1 confers constitutive Nrf2 activation and resistance to chemotherapy in gall bladder cancer. Gastroenterology 2008;135:1358–68.
17. Ohta T, Iijima K, Miyamoto M, et al. Loss of Keap1 function activates Nrf2 and provides advantages for lung cancer cell growth. Cancer Res 2008;68:1303–9.
18. Singh A, Misra V, Thimmulappa RK, et al. Dysfunctional KEAP1-2 interaction in non-small-cell lung cancer. PLoS Med 2006;3:e420.
19. Sjöblom T, Jones S, Wood LD, et al. The consensus coding sequences of human breast and colorectal cancers. Science 2006; 314:268–74.
20. Lee DF, Kuo HP, Liu M, et al. KEAP1 E3 ligase-mediated downregulation of NF-κB signaling by targeting IKKβ. Mol Cell 2009;36:131–40.
21. Hu Z, Lin D, Yuan J, et al. Overexpression of osteopontin is associated with more aggressive phenotypes in human non-small cell lung cancer. Clin Cancer Res 2005;11:4646–52.
22. Dai J, Peng L, Fan K, et al. Osteopontin induces angiogenesis through activation of PI3K/AKT and ERK1/2 in endothelial cells. Oncogene 2009;28:3412–22.
23. Chung CH, Parker JS, Karaca G, et al. Molecular classification of head and neck squamous cell carcinomas using patterns of gene expression. Cancer Cell 2004;5:489–500.
24. Tomida S, Koshikawa K, Yatabe Y, et al. Gene expression-based, individualized outcome prediction for surgically treated lung cancer patients. Oncogene 2004;23:5360–70.
25. Peng T, Golub TR, Sabatini DM. The immunosuppressant rapamycin mimics a starvation-like signal distinct from amino acid and glucose deprivation. Mol Cell Biol 2002;22:5575–84.
26. Sancak Y, Peterson TR, Shaul YD, et al. The Rag GTPases bind raptor and mediate amino acid signaling to mTORC1. Science 2008; 320:1496–501.
27. Carracedo A, Ma L, Teruya-Feldstein J, et al. Inhibition of mTORC1 leads to MAPK pathway activation through a PI3K-dependent feedback loop in human cancer. J Clin Invest 2008; 118:3065–74.
28. Sun SY, Rosenberg LM, Wang X, et al. Activation of Akt and eIF4E survival pathways by rapamycin-mediated mammalian target of rapamycin inhibition. Cancer Res 2005;65:7052–8.
29. Okawa H, Motohashi H, Kobayashi A, et al. Hepatocyte-specific deletion of the keap1 gene activates Nrf2 and confers potent resistance against acute drug toxicity. Biochem Biophys Res Commun 2006; 339:79–88.
30. Yates MS, Tran QT, Dolan PM, et al. Genetic versus chemoprotective activation of Nrf2 signaling: overlapping yet distinct gene expression profiles between Keap1 knockout and triterpenoid-treated mice. Carcinogenesis 2009;30:1024–31.
31. Mootha VK, Lindgren CM, Eriksson KF, et al. PGC-1α-responsive genes involved in oxidative phosphorylation are coordinately downregulated in human diabetes. Nat Genet 2003;34:267–3.
32. Wullschleger S, Loewith R, Hall MN. TOR signaling in growth and metabolism. Cell 2006;124:471–84.
33. Ma XM, Blenis J. Molecular mechanisms of mTOR-mediated translational control. Nat Rev Mol Cell Biol 2009;10:307–18.
34. Kim E, Goraksha-Hicks P, Li L, et al. Regulation of TORC1 by Rag GTPases in nutrient response. Nat Cell Biol 2008;10:935–45.
35. Nardella C, Chen Z, Salmena L, et al. Aberrant Rheb-mediated mTORC1 activation and Pten haploinsufficiency are cooperative oncogenic events. Genes Dev 2008;22:2172–7.
36. Jiang H, Vogt PK. Constitutively active Rheb induces oncogenic transformation. Oncogene 2008;27:5729–40.
37. Meylan E, Dooley AL, Feldser DM, et al. Requirement for NF-κB signalling in a mouse model of lung adenocarcinoma. Nature 2009;462:104–7.
38. Sabatini DM. mTOR and cancer: insights into a complex relationship. Nat Rev Cancer 2006;6:729–34.

39. Engelman JA. Targeting PI3K signalling in cancer: opportunities, challenges and limitations. Nat Rev Cancer 2009;9:550–62.
40. Konstantinidou G, Bey EA, Rabellino A, et al. Dual phosphoinositide 3-kinase/mammalian target of rapamycin blockade is an effective radiosensitizing strategy for the treatment of non-small cell lung cancer harboring K-RAS mutations. Cancer Res 2009;69:7644–52.
41. Liu TJ, Koul D, LaFortune T, et al. NVP-BEZ235, a novel dual phosphatidylinositol 3-kinase/mammalian target of rapamycin inhibitor, elicits multifaceted antitumor activities in human gliomas. Mol Cancer Ther 2009;8:2204–10.
42. Serra V, Markman B, Scaltriti M, et al. NVP-BEZ235, a dual PI3K/mTOR inhibitor, prevents PI3K signaling and inhibits the growth of cancer cells with activating PI3K mutations. Cancer Res 2008;68:8022–30.
43. Coppola D, Szabo M, Boulware D, et al. Correlation of osteopontin protein expression and pathological stage across a wide variety of tumor histologies. Clin Cancer Res 2004;10:184–90.
44. Hofmann HS, Hansen G, Richter G, et al. Matrix metalloproteinase-12 expression correlates with local recurrence and metastatic disease in non-small cell lung cancer patients. Clin Cancer Res 2005;11:1086–92.
45. Kerkelä E, Ala-aho R, Klemi P, et al. Metalloelastase (MMP-12) expression by tumour cells in squamous cell carcinoma of the vulva correlates with invasiveness, while that by macrophages predicts better outcome. J Pathol 2002;198:258–69.
46. Ebi H, Tomida S, Takeuchi T, et al. Relationship of deregulated signaling converging onto mTOR with prognosis and classification of lung adenocarcinoma shown by two independent in silico analyses. Cancer Res 2009;69:4027–35.